Available online at www.sciencedirect.com
SCIENCE DIRECT®
Agricultural Systems 89 (2006) 272–298
AGRICULTURAL SYSTEMS
www.elsevier.com/locate/agsy

Methodology to link production and environmental risks of precision nitrogen management strategies in corn

K.R. Thorp [a,*], W.D. Batchelor [a], J.O. Paz [a], B.L. Steward [a], P.C. Caragea [b]

[a] *Department of Agricultural and Biosystems Engineering, 124 Davidson Hall, Iowa State University, Ames, IA 50011, USA*
[b] *Department of Statistics, 125 Snedecor Hall, Iowa State University, Ames, IA 50011, USA*

Received 17 January 2005; received in revised form 7 September 2005; accepted 23 September 2005

Abstract

A new decision support system called Apollo, which runs the CERES-Maize crop growth model, was used to study the corn (*Zea mays L.*) yield response and the nitrogen (N) dynamics of a cornfield in central Iowa, USA. The model was calibrated to minimize error between simulated and measured yield over five growing seasons. Model simulations were then completed for 13 spring-applied N rates in each of 100 grid cells with varying soil properties. For each N rate and grid cell, simulations were repeated for 37 years of historical weather information collected near the study site. Model runs provided the crop yield and unused N in the soil at harvest for all combinations of N rate, grid cell, and weather year. Using these simulated datasets, a methodology involving cumulative probability distributions was developed such that the yield and unused N resulting from each N rate applied in each grid cell could be directly linked according to their probability of occurrence over the 37 simulated growing seasons. These cumulative probability distributions were used to evaluate the economic and environmental risks of two alternate precision N management strategies for the study area. In the first strategy, N rates were selected to maximize the producer's marginal net return in each grid cell. The environmental cost of this management strategy, in terms of N left behind, was determined to be

* Corresponding author. Tel.: +1 515 294 7350; fax: +1 515 294 2552.
E-mail address: kthorp@iastate.edu (K.R. Thorp).

0308-521X/$ - see front matter
doi:10.1016/j.agsy.2005.09.005

56.2 kg ha^{-1} on average over all grid cells. In the second strategy, N rates were selected to insure that the amount of N left in the soil at harvest would not exceed 40 kg ha^{-1} in 80% of growing seasons. The producer's opportunity cost for reducing N rates to achieve this environmental objective was calculated to be \$48.12 ha^{-1} on average over all grid cells. The overall goal of this work was to develop a methodology for directly contrasting the production and environmental concerns of N management in agricultural systems. In this way, N management plans can be designed to achieve a proper balance between production and environmental goals.

Keywords: Corn; Yield; Nitrogen; Nitrate leaching; Crop modeling; Variable-rate; Prescriptions

1. Introduction

With the increased use of yield monitors on grain combines in the past decade (Searcy et al., 1989), crop yield has repeatedly been shown to exhibit substantial spatial variation across individual fields (Jaynes and Colvin, 1997). In addition, airborne and satellite remote sensing imagery has shown similar variation in crop growth and development throughout the growing season (GopalaPillai and Tian, 1999). Such datasets have demonstrated the potential for variable-rate applications of nitrogen (N) fertilizer, based on the site-specific crop need.

Applying N fertilizer site-specifically also makes sense from an environmental perspective. Bakhsh et al. (2000) identified several properties of the agricultural landscape that altered its susceptibility to movement and loss of nitrate-nitrogen (NO_3-N). These include soil type, topography, soil moisture, tile drainage, and tillage practices. Thus, a robust method for determining appropriate N application rates must consider the spatial variability of the agricultural landscape's NO_3-N loss risk, as well as the spatial variability of the crop's N need. In this way, N prescriptions can be tailored to address both production and environmental concerns.

In addition to the spatial aspects of N management, there is also a complex temporal problem that arises due to the unpredictable nature of weather patterns. Precipitation events drive the movement of NO_3-N through the agricultural system, and rainfall is necessary for the crop to uptake NO_3-N from the soil. However, problems arise when precipitation events, NO_3-N availability, and crop need do not coexist in time (Dinnes et al., 2002). For example, in the midwestern United States, N is most commonly applied in the fall or spring, prior to planting corn. Nitrogen applied at these times has the greatest potential for loss to the environment, because snow melt and heavy rains in the spring season can move NO_3-N out of the agricultural system prior to crop uptake. A similar problem exists during seasons of drought. For this case, suppose NO_3-N is made available through side-dress applications of N fertilizer at mid-season. Although NO_3-N is now available during the time of peak N demand, the lack of water prevents the crop from removing all the NO_3-N from the soil. The excess NO_3-N is then available for loss during precipitation events that occur after harvest, when the crop no longer needs it. Unfortunately, when making N management decisions, knowledge of future weather patterns and precipitation events is

limited to the accuracy of seasonal forecasts. However, large sets of historical weather data now exist for many portions of the world, and these datasets can be used as an indicator of probable future weather patterns for an area. In this way, historical weather data becomes a useful set of information for the development of N management strategies that are conscious of the influence of weather patterns on NO_3-N movement through the agricultural system.

Over the past decade, researchers have focused on a wide variety of methods for developing site-specific N prescriptions. An arsenal of sensing techniques has been employed for identifying N deficient areas of crops, including airborne and satellite remote sensing (Blackmer et al., 1996; Flowers et al., 2003), multispectral camera systems on ground vehicles (Noh et al., 2003), and chlorophyll meter readings of individual corn leaves (Schepers et al., 1992). Although these sensing techniques have successfully identified N deficiencies, they do not effectively account for the spatially varying properties of the agricultural landscape or weather patterns that affect NO_3-N losses from the agricultural system. Other researchers have attempted to develop yield response functions by regressing crop yield against soil nutrient measurements, such as late-spring NO_3-N concentration (Katsvairo et al., 2003) and soil organic matter (Schmidt et al., 2002). High r^2 values for the relationship between crop yield and soil nutrient levels have not been consistently obtained with this approach, because the temporal aspects of N movement through the agricultural system cannot be adequately characterized by a single equation. As a result, soil nutrient concentrations based on point-in-time measurements have not been helpful for developing variable-rate N recommendations. The greatest limitation in these approaches is that none of them can adequately account for the fact that N movement depends heavily on the temporal pattern of weather encountered during the growing season.

The CERES-Maize crop growth model (Jones and Kiniry, 1986) is another tool that has been used to study precision N management for corn (*Zea mays* L.) (Paz et al., 1999; Batchelor et al., 2002). This model utilizes carbon, N, and water balance principles to simulate, in homogenous units, the daily processes that occur during plant growth and development. The final corn yield for the simulated growing season is then calculated on the harvest date. The model has been shown to adequately simulate corn growth, development, and yield on plot-level, field-level, and regional scales for many locations around the world. Inputs required for model execution include management practices (plant genetics, plant population, row spacing, planting and harvest dates, and fertilizer application amounts and dates), environmental factors (soil type, drained upper limit, lower limit, saturated hydraulic conductivity, root weighting factor, and effective tile drain spacing), and weather conditions (daily minimum and maximum temperature, solar radiation, and precipitation). Since CERES-Maize utilizes N balances for crop growth analysis, it can be conveniently extended to calculate surface and subsurface NO_3-N losses. For example, the model has undergone several modifications such that NO_3-N in run-off (Gabrielle et al., 1995), tile flow (Garrison et al., 1999), and leaching (Gabrielle and Kengni, 1996) can be simulated as part of the crop production process. Since CERES-Maize can collectively account for many of the spatial and temporal factors that affect crop yield and N movement through the agricultural system, it serves as a very useful

and appropriate tool for developing N management strategies that address both the economic and the environmental concerns of corn production.

A new decision support system called Apollo runs CERES-Maize and other DSSAT crop models for management zones within a field (Batchelor et al., 2004). Apollo is an interface that can be used to calibrate and validate model parameters and execute model runs to achieve a variety of precision farming objectives, such as prescription analysis and yield gap analysis. In this work, the Apollo system was used to calibrate CERES-Maize and run N prescriptions for an Iowa cornfield divided into 100 grid cells.

The overall objective was to use the results of the prescription simulations to develop a methodology for estimating the economic and environmental trade-offs of N management strategies for this cornfield. The existence of a trade-off between the production and environmental concerns of N management is an important concept, because of the dual opposing role that N plays in crop production and environmental quality. Whereas N fertilizer is beneficial for maximizing crop production, unused N fertilizer that is lost from the agricultural system poses a threat to environmental quality, wildlife welfare, and human health. Therefore, N management strategies of the future must aim to find the appropriate balance between these opposing concerns. The first step in this endeavor is to develop a methodology for predicting how a particular N management strategy will affect corn yield and unused N remaining in the soil at harvest. With such a methodology, N management strategies can be developed and implemented with a direct understanding of the cost to the producer and the cost to the environment. In addition, the methodology could aid in the development of environmental legislation and producer compensation programs that aim to reduce the environmental risk of agricultural N management.

2. Methods

2.1. Data preparation

The study area included a 20.25 ha section of a production cornfield near Perry, IA, USA (41.93080°N, 94.07254°W). This area was divided into 100 grid cells, each 45 m by 45 m in size. A digitized soil survey indicated that five primary soil types were present in the study area: Canisteo silty clay loam, Clarion loam, Nicollet loam, Harps loam, and Okoboji silty clay loam. Estimates of the physical properties for these soils were obtained from two sources. Ratliff et al. (1983) provided the drained upper limit (DUL) ($cm^3\ cm^{-3}$) and lower limit for various soil textures. In addition, values for the saturated hydraulic conductivity (K_{SAT}) ($cm\ d^{-1}$), bulk density (BD) ($g\ cm^{-3}$), and soil pH at various soil depths were obtained from the county soil survey (USDA-SCS, 1981). Saturated moisture content (SAT) ($cm^3\ cm^{-3}$) was calculated from BD using

$$\mathrm{SAT} = 0.92^{*}\left(1 - \frac{\mathrm{BD}}{2.65}\right). \tag{1}$$

Each of the 100 grid cells was assigned the soil properties for the soil type that covered the largest area within the grid cell (Fig. 1). A Visual Basic for Applications (VBA) script was created within the ArcGIS 8.2 software to create the grid layout, clip the digital soil survey by grid cell, determine the soil type covering the largest area, and write the soil parameters to a soil file for crop model runs (Thorp et al., 2005a). This soil file was used for both the model calibration and the N rate prescription simulations.

Five seasons of measured corn yield were available for crop model calibration. Measured yield datasets were obtained using a yield monitor on a grain combine during the 1994, 1996, 1998, 2000, and 2002 growing seasons. The VBA script in ArcGIS was extended to clip the yield data by grid cell, calculate the average yield for each grid cell, and write the yield files to a disk. The yield files were used to compare measured and simulated yield during the model calibration phase.

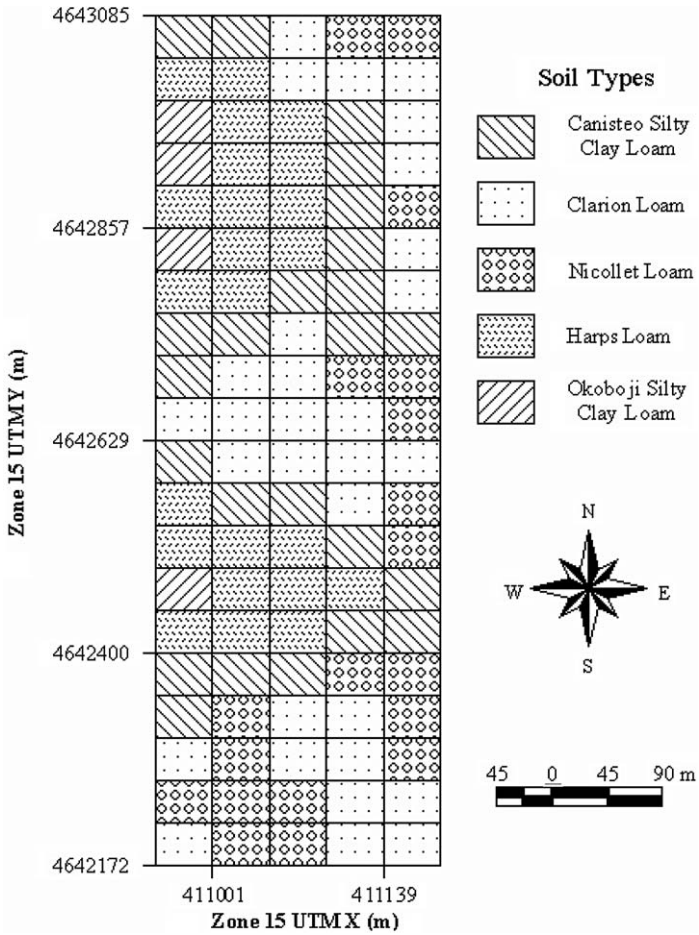

Fig. 1. Soil types for the 20.25 ha study area divided into 100 grid cells.

Weather files were created based on the availability of 37 years of historical weather data collected near Perry, IA. These historical weather datasets allowed for the simulation of N rate performance over the weather conditions of the past 37 growing seasons. In addition, weather information for 5 of the 37 growing seasons was used in the model calibration. For years 1966 to 1995, weather data was collected at the Perry grain elevator, 10 km from the study site. This data was obtained from a historical weather database maintained by the Department of Agronomy at Iowa State University (http://mesonet.agron.iastate.edu). For years following 1995, weather data was collected using a weather station directly at the site.

Soil water content, initial nutrient levels, and plant population were not available for this site. Appropriate values were assumed and assigned uniformly to each grid cell across the study area. In addition, since individual growing seasons were simulated independently, initial conditions were specified uniformly for each growing season and carry over of soil water and nutrients between growing seasons was ignored. Initial soil water content for each simulation was set to 0.3 $cm^3\ cm^{-3}$, a value just below the DUL for the soils in the field. Initial N levels were set arbitrarily to 0.1 g elemental N per Mg soil. For the purpose of this study, it was assumed that the soil profile contained only a negligible amount of N at the beginning of the season. In practice, a producer would subtract pre-season soil nutrient levels from the N fertilization rate recommendations generated with the simulation methodology developed in this work. Finally, plant population was set to 7.4 plants m^{-2} based on the average of population measurements collected during the 1996 growing season. These approximations for soil water content, initial nutrient levels, and plant population were used for both the model calibration phase and for the N rate prescription simulation phase.

Management practice model inputs were changed between the model calibration phase and the N rate prescription simulation phase. To calibrate the model, the producer's actual planting date, actual harvest date, and actual fertilizer application rates and dates were used for each of the 5 growing seasons available for calibration. For the N rate prescription simulations, the planting and harvest dates were assumed to be uniform across all 37 growing seasons. In this case, the dates of planting and harvest were set to April 25 and October 12, respectively, based on the average of the 5 years of known management practice dates for this producer and study site. Also, the model was set to apply all N on April 15 in each of the 37 seasons included in the prescription simulations. Values for N rate were left blank in the model input file, such that the Apollo decision support system could alternatively input various N rates to test during the N prescription simulations.

2.2. Model calibration

Paz et al. (1999) developed a technique to calibrate the CERES-Maize crop growth model for tile-drained soils in the Midwestern United States. The technique implements the simulated annealing algorithm to adjust model input parameters to minimize the error between measured and simulated yield within an area

of interest. In this work, this technique was implemented within the Apollo calibration module to calibrate two CERES-Maize model parameters: K_{SAT} of the deep impermeable layer and effective tile drainage rate. Although a first estimate of the K_{SAT} value was obtained from the county soil survey, the range of parameter values for most soil types in the survey is very wide. The calibration procedure served to fine-tune this parameter to more accurately represent the water table dynamics of each grid cell. If a grid cell was properly drained, the calibration procedure generated a large value for the K_{SAT} parameter. In this case, excess water is more quickly lost out the bottom of the profile and water tables are kept low or never form, which allow roots to grow deep in the soil profile. The calibration procedure would give small values for the K_{SAT} parameter if a grid cell was poorly drained. This causes water to move more slowly through the bottom soil layer, water tables are kept high, and roots grow to more shallow depths within the soil profile. The effective tile drainage rate controls the speed at which water is lost through tile lines when the water table is above the tile. For each of the 100 grid cells at the study site, the technique of Paz et al. (1999) was used to solve for the optimum set of the two model parameters that minimized the root mean square error (RMSE) between simulated and measured yield for the five available seasons of measured yield data. Parameters were calibrated uniquely for each grid cell to account for spatial variability within the field. The objective function to be minimized during model calibration with the simulated annealing algorithm can be written as

$$\mathrm{RMSE}_i = \left(\frac{1}{n} \cdot \sum_{j=1}^{n} (Ym_{i,j} - Ys_{i,j})^2 \right)^{0.5}, \tag{2}$$

where $Ym_{i,j}$ is the measured yield and $Ys_{i,j}$ is the simulated yield in the ith grid cell for the jth of n seasons of yield data. The model calibration procedure in Apollo provided the final minimized RMSE between measured and simulated yield for each grid cell, which represents the error associated with optimizing the two soil parameters within the grid cells over the five calibration growing seasons. These RMSE values also serve as a performance indicator for the calibration procedure, where a RMSE of less than 1000 kg ha^{-1} is roughly less than 10% error. After completing a satisfactory calibration with acceptable RMSE values, the calibrated model parameters for each grid cell were used in an N prescription analysis within the Apollo software.

Model validation is important for providing evidence that a calibrated model is performing sensibly for calibration-independent datasets. Such model testing procedures were especially important for this work because model calibration was carried out using data from only five growing seasons, and the calibrated model was then used to simulate crop yield and unused N for an extended set of historical weather over 37 growing seasons. Thus, the later simulations will only perform as well as the calibration has successfully captured the key drivers of the observed spatial variability. The details concerning model validation at this study site have been explored and presented in previous work (Thorp et al., 2005b).

2.3. Nitrogen prescription analysis

Prescription analyses in Apollo use three nested loops to simulate crop yield and N pooling for a set of N rates, management zones, and historical weather years. First, Apollo loops through a series of user-defined N rates, running CERES-Maize each time to assess the yield response and N pools for each N rate. To facilitate simulation of fall, spring, and side-dress applications, the user can also specify the fertilizer application date. A second nested loop repeats the process for each user-defined management zone or grid cell, and the third loop repeats the entire process for all the available years of historical weather data for the field location. Thus, the Apollo prescription module calculates information useful for studying yield response and N pools, as if precision N management strategies had been used during the weather patterns of previous growing seasons. In order to develop N management strategies for the future, we simulate and analyze how N rates would have performed in the past.

The Apollo prescription module was run for the study site to simulate the crop yield response and the amount of N in four pools, including NO_3-N in the soil at harvest, NH_4 in the soil at harvest, total NO_3-N leached, and total NO_3-N lost out the tile. The four N pools were summed to generate a value for total unused N at the end of the growing season. Model simulations were run for 13 N application rates over 37 years of historical weather data near the study site (1966–2002). Simulated N rates ranged from 80 to 320 kg ha^{-1} at increments of 20 kg ha^{-1}. While running the prescription analysis, Apollo generated a text file containing the simulation results for all combinations of N rates, grid cells, and weather years. Thus for this work, the prescription output file contained 48,100 entries (13 rates * 37 years * 100 grid cells).

2.4. Cumulative probability distributions

Prescription analyses in Apollo have the potential to generate a very large amount of simulated data, depending on the number of grid cells, N rates, and weather years used in the simulation. To condense this dataset for interpreting the effect of historical weather patterns on N mobility in the agricultural system, a methodology involving cumulative probability distributions, which give the probability that a variable takes a value lesser than or equal to a specified quantity, was developed. Two families of cumulative probability curves were calculated for each grid cell: one for yield and the other for unused N left in the soil at harvest. The first family provides the cumulative probability of yield for each N rate over the number of weather years, 37 in this case. Each curve in this family represents the probability of obtaining crop yield by applying the associated rate of N fertilizer consistently over a 37-year period. The second family gives the cumulative probability of unused N for each N rate over the number of weather years. Each curve in this family represents the probably, or risk, of leaving unused N in the soil when applying the associated N rate consistently over a 37-year period. Using these two families of cumulative probability distributions together, the economic and environmental costs of applying various N

rates can be compared, and N rates can be selected to accomplish objectives associated with both crop production and environmental protection. Because the two families of curves are unique for each grid cell, the complete set of curves for all grid cells can be used to develop variable-rate N management plans that achieve the production or environmental objectives for the entire field. It is convenient to fit probability distributions to the data generated from historical weather simulations, because the dataset will ultimately be used to develop N fertilizer recommendations for future growing seasons in which weather conditions are unknown. By fitting probability distributions to the simulated data for yield and unused N for past weather years, the effect of unknown weather patterns on future yield and unused N can be characterized in terms of chance or probability. Thus, N recommendations can be designed with a level of certainty that a given yield threshold will be achieved or that an unused N threshold will not be exceeded.

To proceed with this analysis, a Visual Basic application was written to manipulate the data within the Apollo prescription file and to fit appropriate probability distributions. Automation of this process within Visual Basic was important because of the large number of datasets to which distributions were fitted. Distributions were fit for both yield and unused N for each N rate in each grid cell (2 variables * 13 rates * 100 grid cells = 2600 distributional fits). Initial work focused on fitting normal probability distributions to both the yield and unused N datasets. However, further investigations using histograms and the Shapiro-Wilk test (Shapiro and Wilk, 1965; Royston, 1995) revealed that the datasets were oftentimes severely non-normal.

In an effort to remedy this problem, several alternative distributions were explored. Based on the results of χ^2 goodness-of-fit tests and visualization of distributions fitted to histograms, the beta probability distribution was chosen for use with the simulated yield data and the exponential probability distribution was selected for use with the simulated data for unused N.

The flexibility of the beta distribution proved to be helpful for fitting the heavily skewed simulated yield datasets in this research. The general formula for the probability density function of the beta distribution is

$$f(x) = \frac{(x-a)^{p-1}(b-x)^{q-1}}{B(p,q)(b-a)^{p+q-1}}, \quad a \leqslant x \leqslant b,\ p > 0,\ q > 0, \tag{3}$$

where p and q are shape parameters, a and b are the respective upper and lower bounds of the distribution, and $B(p,q)$ is the beta function (Johnson et al., 1994). The beta function is

$$B(p,q) = \int_0^1 t^{p-1}(1-t)^{q-1}\mathrm{d}t. \tag{4}$$

To fit a beta distribution, all four parameters, p, q, a, and b, must be estimated. In this work, the lower bound, a, was assumed to be 0 for all yield datasets, since yield cannot be negative. The three remaining parameters were estimated using a combination of maximum likelihood and method of moments estimation in an iterative procedure, all implemented within the Visual Basic algorithm. Initially, the upper

limit, b, was set to the largest value in each yield dataset. Next, the method of moments estimators (Johnson et al., 1994) for both p and q were calculated. All four parameters were then used to compute the value of the likelihood function for the beta distribution (Gnanadesikan et al., 1967). This process was iterated several hundred times while incrementing the value of b by one in successive iterations. The values of p, q, a, and b that gave the maximum value for the likelihood function were assumed to be the parameters that provided the best fit of Eq. (3) to a given yield dataset. A unique set of distributional parameters was calculated for each of the 2600 histograms of simulated yield data. These parameters were then used to calculate the cumulative beta probability distribution for each yield dataset. The cumulative beta probability distribution, also known as the incomplete beta function ratio, can be expressed as

$$I_x(p,q) = \frac{\int_0^x t^{p-1}(1-t)^{q-1}\mathrm{d}t}{B(p,q)}, \quad 0 \leqslant x \leqslant 1,\ p > 0,\ q > 0, \tag{5}$$

(Johnson et al., 1994). This equation restricts the lower and upper bound to 0 and 1, respectively. Therefore, the parameter values, a and b, were used to scale each yield data value down to within this required range. To solve the beta function (Eq. (4)) and the incomplete beta function ratio (Eq. (5)) for each yield dataset, numerical approximations, translated from the C programming language, were incorporated into the Visual Basic algorithm (Press et al., 1992).

Histograms of the simulated datasets for unused N in the soil at harvest suggested that an exponential distribution would provide an appropriate fit. The probability density function of the exponential distribution can be written as

$$f(x) = \frac{1}{\beta}\mathrm{e}^{-(x-\mu)/\beta}, \quad x \geqslant \mu,\ \beta > 0, \tag{6}$$

where μ is a location parameter and β is a scale parameter. The location parameter for all exponential distributions was set such that the lower asymptote was equal to the smallest value for unused N in the dataset. As a result, parameter estimation was much simpler for the exponential distribution compared to the beta distribution, because estimation of only one parameter, β, was required, and the maximum likelihood estimator of β is simply the sample mean. The cumulative exponential distribution function can be expressed as

$$F(x) = 1 - \mathrm{e}^{-(x-\mu)/\beta}, \quad x \geqslant \mu,\ \beta > 0, \tag{7}$$

(Johnson et al., 1994). A short segment of code was written to calculate the cumulative exponential distributions for each of the 2600 sets of simulated unused N datasets and added to the Visual Basic application.

2.5. Nitrogen management decisions

The families of cumulative beta probability distributions for yield and the families of cumulative exponential distributions for unused N at harvest were used to assess the economic and environmental consequences associated with N management

decisions. A comparison of two N management strategies was carried out to demonstrate how the distributions could be used. The objective of the first N management strategy was to maximize the profitability of the management practice for the producer. Paz et al. (1999) presented a simple equation to calculate marginal net return for N fertilizer management in corn:

$$\text{Marginal net return} = Y \cdot P_c - N \cdot P_n, \tag{8}$$

where Y is the corn yield (kg ha^{-1}), P_c is the price of corn (\$ kg^{-1}), N is the N application rate (kg ha^{-1}), and P_n is the price of N fertilizer (\$ kg^{-1}). For this study, P_c was set to \$0.086 kg^{-1} and P_n was set to \$0.46 kg^{-1}, which are current market values for corn and N fertilizer in Iowa. Managing N to optimize long-term marginal net return assures that producers can achieve the maximum possible profit from their corn crop. However, this practice has been shown to have significant environmental implications (Burkart and James, 1999; Goolsby et al., 2001), because unused NO_3-N is highly susceptible to loss from the agricultural system. Therefore, the objective of the second N management strategy was to reduce the level of applied N to achieve an environmental objective: leave less than 40 kg ha^{-1} of N in soil at harvest with a probability of 80%. Because the two families of cumulative probability curves link yield to unused N in the soil at harvest, they allow for the quantification of any production losses that a producer might incur for managing N at levels below the production optimal. In this way, the producer's opportunity cost for applying reduced N rates can be calculated by extending Eq. (8)

$$\text{Opportunity cost} = (Y_{max} - Y_{red}) \cdot P_c - (N_{max} - N_{red}) \cdot P_n, \tag{9}$$

where Y_{max} and N_{max} are the yield achieved and N rate used when maximizing net return and Y_{red} and N_{red} are the reduced yield and reduced N rate for managing N to achieve the environmental objective. For the purpose of introducing this methodology, the analysis was described in detail using grid cell #4 as an example. By then repeating the analysis for all 100 grid cells, two variable-rate N prescription maps were generated for the study area: one for maximizing the producer's net return and the other for accomplishing the environmental objective.

3. Results

3.1. Calibration results

Cell-level differences between measured and simulated yield as indicated by RMSE ranged from 50 to 1075 kg ha^{-1} with an average RMSE of 490 kg ha^{-1} across all grid cells (Fig. 2). The average RMSE for grid cells dominated by the Canisteo, Clarion, Nicollet, Harps, and Okoboji soil types were 406, 649, 404, 472, and 318 kg ha^{-1}, respectively. Errors for grid cells dominated by Clarion loam were greater on average than that of the other soil types, indicating that the model had more difficulty explaining yield variability in grid cells having this soil type. Clarion loam is a gently sloping, well-drained soil on convex upland knolls (USDA-SCS,

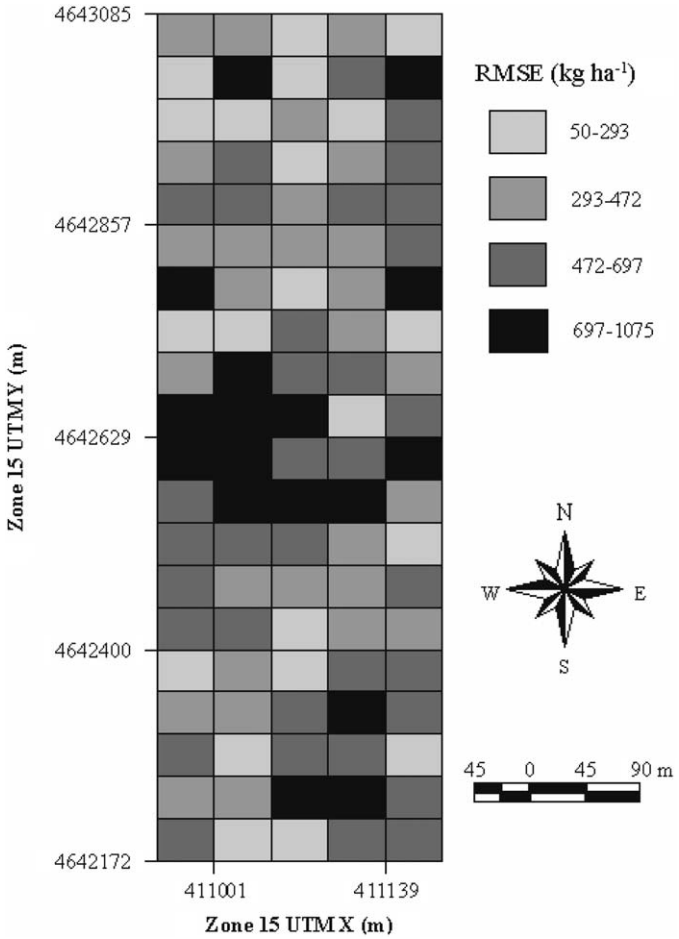

Fig. 2. Root mean square error for the two-parameter calibration in each grid cell.

1981), meaning the soil type is generally present on the sideslopes of the swell and swale topography typical of the central Iowa countryside. Therefore, a possible explanation for the greater average RMSE in Clarion grid cells is that the model does not adequately account for surface run-on and sub-surface water flow between neighboring grid cells, the dynamics of which would be more significant for a sloped topography. Another interesting note is that the aggregation of high RMSE grid cells across the center of the field corresponds to the location of the north sideslope of a well-defined gully that cuts through the study area. These results also suggest that model calibration performance is spatially linked to topography. Errors for grid cells dominated by the Okoboji silty clay loam were significantly lower than that of the other soil types. Okoboji silty clay loam is a very poorly drained soil occurring in concave depressions on uplands (USDA-SCS, 1981). Low RMSE values for the

Okoboji dominated grid cells indicate that the model performed well in mimicking the water flow dynamics in these poorly drained areas.

The map of cell-level calibration errors (Fig. 2) is useful for assessing the spatial distribution of RMSE across the study area; however, the RMSE associated with an individual growing season in the calibration dataset is lost during the averaging process of the RMSE calculation (Eq. (2)). In order to visualize the error associated with individual growing seasons, a one-to-one plot of simulated versus measured yield was constructed (Fig. 3). This plot illustrates the relationship between measured and simulated yield for each of the five calibration years and for each of the 100 grid cells, where the vertical distance between an individual data point and the one-to-one line represents the difference between measured and simulated yield. Cell-level yield for the 1994, 1998, and 2002 growing seasons tended to cluster at 10,600 kg ha^{-1}; however, deviations from the one-to-one line are more apparent for the 1998 and 1994 seasons than for the 2002 growing season. Cell-level yield during the 1996 and 2000 growing seasons tended to cluster around 9250 and 7500 kg ha^{-1}, respectively. These lower yielding growing seasons improved the ability of the model to explain year-to-year variation by increasing the yield range in the calibration dataset. Overall, the model was able to explain much of the yield variability ($r^2 = 0.89$) when considering all 100 grid cells and all five growing seasons used for calibration (Table 1). The strength of linear regression was reduced when considering the fit for any individual year, because the cell-level yields for single seasons years tended to cluster together in relatively narrow ranges (Fig. 3). However, RMSE calculations for any given production year showed that deviations between field-level measured and simulated yields were not greater than 600 kg ha^{-1} (Table 1). Since past research has supported RMSE and related statistics over correlation-regression analysis for testing crop model

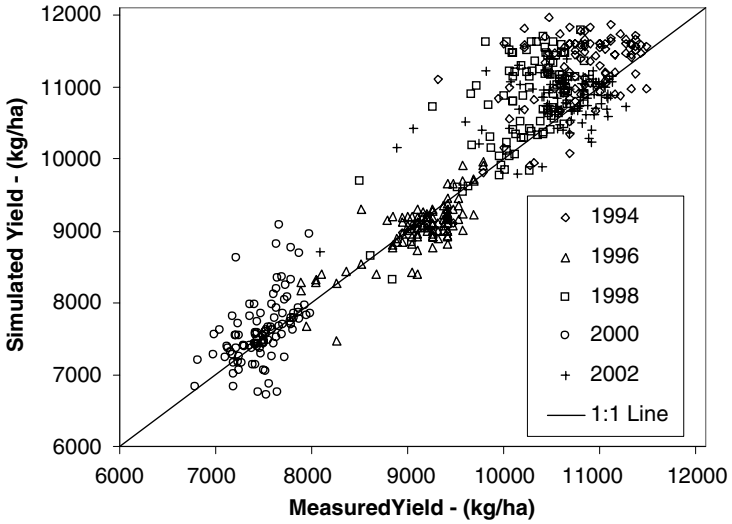

Fig. 3. Simulated versus measured corn yields over 100 grid cells for five growing seasons.

Table 1
Field-level measured versus predicted yield relationships

Production year	Measured yield (kg ha^{-1})	Predicted yield (kg ha^{-1})	RMSE (kg ha^{-1})	r^2
1994	10,788	11,224	520	0.30
1996	9137	9039	217	0.63
1998	10,218	10,773	598	0.47
2000	7484	7617	286	0.26
2002	10,625	10,786	323	0.31
All years	9650	9888	490	0.89

accuracy (Kobayashi and Salam, 2000), it is expected that the lower r^2 values for individual seasons can be ignored in favor of the more descriptive RMSE calculations.

Values for the two optimized parameters, resulting from applying the calibration procedure within each grid cell, were within the expected ranges. The average value for effective tile drainage rate was 0.107 day^{-1} with a standard deviation of 0.059 day^{-1} across 100 grid cells. The minimum value for this parameter was 0.011 day^{-1} in grid cell #29, and the maximum value was 0.246 day^{-1} in grid cell #26. These values fell within the expected range of 0.01 and 0.25 day^{-1} for effective tile drainage rate. The average value for saturated hydraulic conductivity of the deep layer was 0.790 cm day^{-1} with a standard deviation of 0.646 cm day^{-1} across 100 grid cells. The minimum value for this parameter was 0.094 cm day^{-1} in grid cell #83, and the maximum value was 1.976 cm day^{-1} in grid cell #54. These values fell within the expect range of 0.001 and 2 cm day^{-1} for saturated hydraulic conductivity.

3.2. Grid cell #4 example

Two families of cumulative probability distributions were produced for each grid cell. Since it is not feasible to show the resulting 200 graphs, the results of grid cell #4 were selected randomly and presented as an example. The cumulative beta probability distributions of yield for grid cell #4 demonstrate how corn yield and N rate can be related for making N management decisions. For each of the 13 N rates, model simulations provided 37 values for yield in grid cell #4, representing the seasonal corn yield achieved with an N rate given the weather conditions of the past 37 growing seasons. An example histogram for the simulated yield values in grid cell #4 at an N rate of 220 kg ha^{-1} demonstrates how the yield datasets can be well characterized using a beta distribution (Fig. 4). Distributions of simulated yield for other N rates and grid cells typically resembled this histogram in which the lack of an upper tail skewed the distribution heavily to the left. One interpretation of this occurrence is that the weather conditions for most seasons allowed corn yields to approach the potential upper limit for yield in this field. In other seasons when weather conditions were less favorable, simulated yields were significantly lower than the yield potential which created the tapering effect on the left side of the distribution. For this histogram, the four beta parameters, p, q, a, and b, estimated for the fit were 3.60, 0.98, 0.20 and 11,633, respectively. By fitting unique beta distributions to each of

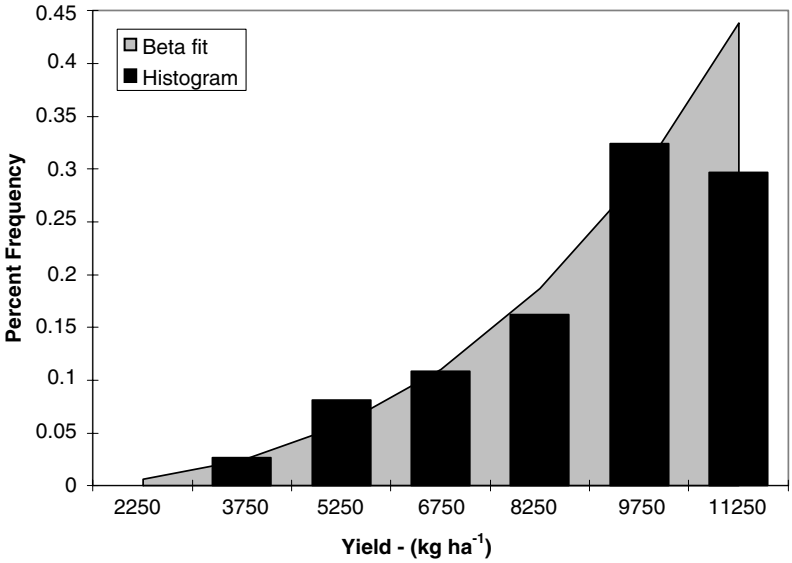

Fig. 4. Histogram of the grid cell #4 simulated yield values over 37 years of historical weather at an N rate of 220 kg ha^{-1} and a fitted beta distribution.

the 13 yield histograms for N rates in grid cell #4 and calculating the cumulative beta probability distribution using the resulting beta parameters, a family of curves that explain the *chance* of corn yield response to N rates given the weather conditions of the past 37 years was generated (Fig. 5). At the time N management decisions are made, these curves are used with the understanding that corn yield response in grid cell #4 will be heavily influenced by the unknown pattern of weather encountered between the N application and harvest. However, based on the patterns of weather seen in previous years, it is possible to describe future corn yield in terms of chance or probability, such that N management decisions can be made less blindly. Cumulative beta probability distributions of yield in grid cell #4 generally showed an increasing trend with N rate at equal probability levels. An exception occurred in the range of the 0% and 20% probability thresholds of yield between 4000 and 8000 kg ha^{-1}. A likely explanation is that small levels of N stress aided root development early in the season, which better prepared the crop to combat water stress and increase yield in these relatively low yielding years. This area of the curve is also perhaps less important, because producers will likely be more interested in yield probabilities much greater than 10%. The beta distribution also has difficulty fitting the high yield end of the histogram in Fig. 4, and the resulting probability curves in Fig. 5 are awkwardly shaped with no roll-off effect in the upper portion of the distribution. These results provide evidence that further analysis may be more accurate if focused away from the tails of the distribution. Finally, the yield distributions for grid cell #4 did not change significantly for N rates above 280 kg ha^{-1}, indicating that yield was not affected by increasing N rates above this level.

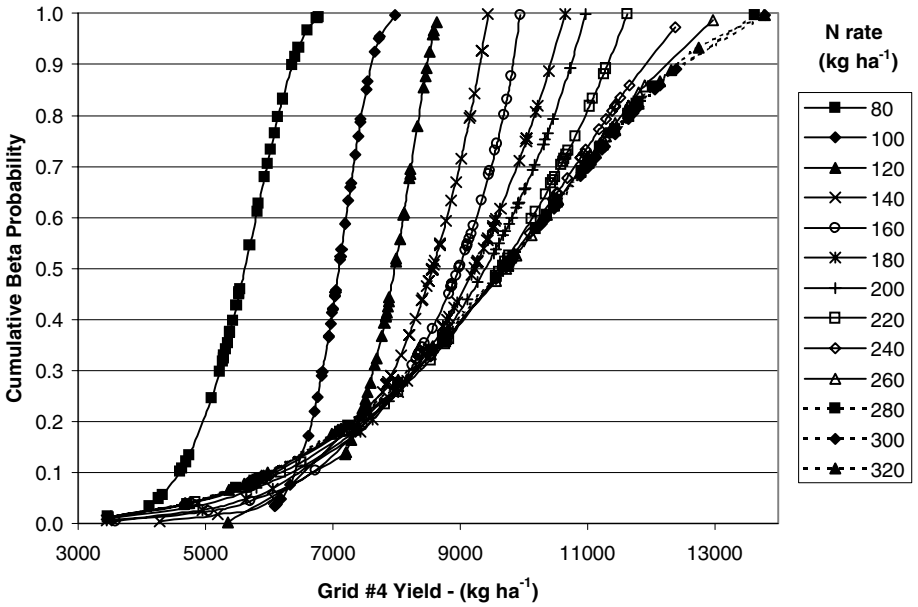

Fig. 5. Cumulative beta probability of yield in grid cell #4 for N rates of 80 to 320 kg ha^{-1}.

Similar to the cumulative beta probability distributions of yield, the cumulative exponential probability distributions of unused N left in the soil at harvest for grid cell #4 demonstrate how unused N and N rate can be related for making N management decisions. For each of 13 N rates, model simulations provided 37 values for unused N in grid cell #4, representing the seasonal post-harvest soil N content obtained with an N rate given the weather conditions of the past 37 growing seasons. An example histogram for the simulated unused N values in grid cell #4 at an N rate of 220 kg ha^{-1} suggests that the unused N datasets can be well characterized using an exponential distribution (Fig. 6). Distributions of unused N for other N rates and other grid cells typically resembled this histogram with a majority of growing seasons having relatively small amounts of N left in the soil, particularly for the lower N rates. In other seasons when weather conditions were not favorable to uptake of N by plants, greater amounts of N were left in the soil and this created the tapering effect on the right side of the distribution. As N rates were increased, the right side of the distribution tended to taper off more slowly. For the histogram in Fig. 6, a value of 13.73 was estimated for the exponential parameter, β. The distribution was adjusted right by a factor of 16.58, the lowest unused N value in the 220 kg ha^{-1} dataset for grid cell #4. Similar to the curves for yield, the cumulative exponential probability distributions of unused N explain the *chance* that different N rates will leave N in the soil at harvest given the weather conditions of the past 37 growing seasons (Fig. 7). This family of curves permits the addition of an environmental component to N management decisions, such that N applications can be designed to achieve a balance between production and environmental goals. Cumulative

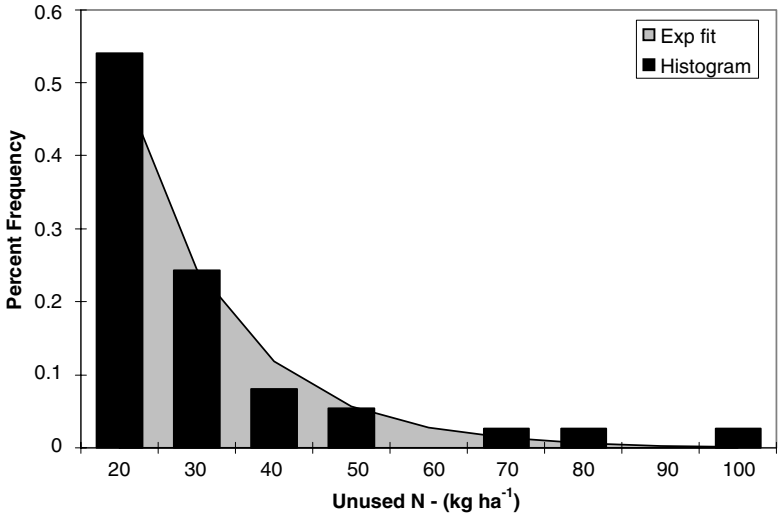

Fig. 6. Histogram of the grid cell #4 simulated unused N values over 37 years of historical weather at an N rate of 220 kg ha^{-1} and a fitted exponential distribution.

exponential probability distributions of unused N for grid cell #4 showed an increasing trend with N rate at equal probability levels. An interesting feature of the unused N probability curves is that, even for the lowest N rate, the simulations always resulted a small amount of N, approximately 15 kg ha^{-1}, left in the soil at harvest. This phenomenon in the simulation results may be attributed to mineralization of N at the end of the growing season after the crop was no longer taking up nutrients, or it may an artifact of the model.

3.3. Statistics over 100 grid cells per N rate

In the process of fitting a distribution and developing cumulative probability curves for yield and unused N, one data dimension, the number of weather years, is essentially removed from prescription simulation datasets. The data can then be described in terms of beta distribution parameters, exponential distribution parameters, and cumulative probability distributions over the two remaining data dimensions, number of N rates and number of grid cells. However, it is not feasible to show the histograms, distributional fits, and cumulative probability curves for every simulated N rate in every grid cell within the study area. Instead, the mean and standard deviation was used to summarize the distribution of estimated beta and exponential parameters at each N level over all 100 grid cells (Table 2). As expected, the prescription simulations showed that an increase in N rate increased yield in grid cells on average, but it also increased the amount of unused N in the soil after harvest. Because yield increased with N rate, the upper limit beta parameter, b, for the yield distributions also increased on average with N rate. Standard deviations for yield, unused N, and b all showed a general increasing trend with N rate. The beta shape

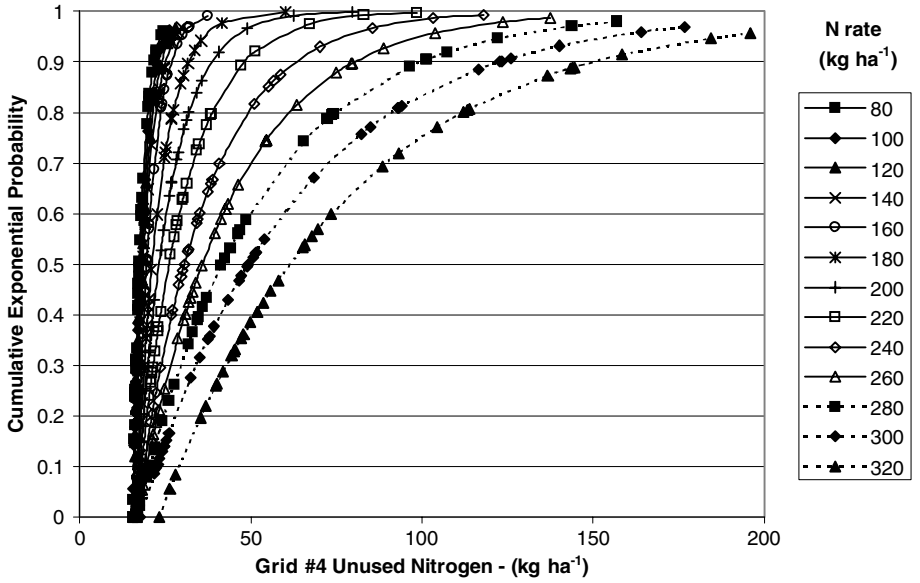

Fig. 7. Cumulative exponential probability of unused N in grid cell #4 for N rates of 80–320 kg ha^{-1}.

parameter, p, showed a decreasing trend with N rate on average across all grid cells. When the N rate increased above 180 kg ha^{-1}, the p parameter was on average approximately 4.0 with a standard deviation of 0.7. The q parameter of the beta distribution decreased from 3.0 at 80 kg ha^{-1} to 0.91 at 160 kg ha^{-1} and then increased to 2.1 as N rate increased to 320 kg ha^{-1}. For the exponential distributions of unused N, the average β parameter across all grid cells and its standard deviation both

Table 2
Summary statistics (average and standard deviation) for the 37-year average yield, beta parameters, the 37-year average unused N, and exponential parameters for each N rate over 100 grid cells

N rate (kg ha^{-1})	Yield (kg ha^{-1})		Beta Parameters						Unused N (kg ha^{-1})		Exponential param.			
			b		p		q				β		Scale	
	Avg	SD	Avg	SD	Avg	SD	Avg	SD	Avg	SD	Avg	SD	Avg	SD
80	5386	228	6985	133	10.7	4.96	3.03	1.30	21.7	3.1	4.4	2.7	17.3	1.3
100	6830	340	8068	163	23.5	15.7	3.82	2.35	22.6	3.9	5.3	3.5	17.3	1.4
120	7604	397	8831	162	19.4	11.8	2.78	1.55	23.6	4.7	6.1	4.4	17.5	1.4
140	8064	434	9460	188	9.53	4.89	1.51	0.76	24.7	5.8	7.1	5.5	17.6	1.4
160	8337	446	9926	114	5.13	2.11	0.91	0.34	26.2	7.0	8.2	6.9	18.0	1.4
180	8522	463	10,553	220	4.28	1.32	0.99	0.29	29.1	8.2	10.9	8.0	18.2	1.4
200	8669	469	10,959	171	3.65	0.84	0.94	0.21	32.8	9.3	14.5	9.2	18.2	1.4
220	8843	501	11,680	237	3.51	0.71	1.12	0.30	37.5	10.7	19.2	10.5	18.3	1.5
240	8982	531	12,407	349	3.59	0.70	1.38	0.37	44.3	12.1	25.7	12.0	18.5	1.4
260	9059	532	13,151	420	3.87	0.64	1.74	0.34	52.3	13.4	33.7	13.3	18.6	1.4
280	9105	532	13,727	555	4.04	0.69	2.05	0.39	61.8	15.0	42.9	14.8	18.9	1.5
300	9131	516	13,891	590	4.04	0.69	2.11	0.40	73.7	16.2	52.8	15.5	20.8	2.1
320	9152	498	13,904	581	4.03	0.68	2.09	0.40	88.2	16.6	62.7	15.4	25.4	4.5

increased with increasing N rate. This was expected since a larger β value makes the exponential distribution decay more slowly, representing an increased frequency of larger amounts of N left unused. For all but the highest two rates, the average location factor for the exponential distribution remained between 17 and 19 with a low standard deviation, indicating most N rates and most grid cells had at least one season with less than 20 kg ha^{-1} N left unused. The spatial distribution of summary statistics similar to those in Table 2 could also be studied by averaging over N rate instead of over grid cells; however, this makes less sense because only one N rate would be applied in a given season. An investigation into the spatial effect of grid cell location will be the subject of the next section, which illustrates the use of the cumulative probability curves to select N rates and develop N prescriptions that satisfy production and/or environmental requirements.

4. Discussion

4.1. Environmental cost of optimizing economic return

For a farming operation to be profitable, producers must use management practices that maximize marginal net return (Eq. (8)). Continuing with the analysis of grid cell #4, calculations were carried out to determine the relationship between N rates and marginal net return. Average marginal net return represents the average return for each N rate over all 37 growing seasons. Maximum and minimum marginal net return represents the greatest and least return achieved with each N rate in a single year. For grid cell #4, an N rate of 240 kg ha^{-1} maximized the average marginal net return over 37 growing seasons (Fig. 8). If the producer applied this rate to grid cell #4 in each year, there would be a 50:50 chance that the marginal net return would be greater than or less than \$689.40 ha^{-1}. However, the uncertainty in marginal net return values for individual seasons is large for the 240 kg ha^{-1} N rate, because the range between minimum and maximum net return values widen significantly at the higher N rates. In one of the 37 years, the 240 kg ha^{-1} N rate may result in a net return of \$953.76 ha^{-1} while in another it may result in a return of only \$188.36 ha^{-1} (Fig. 8). The cumulative beta probability distributions of yield now become useful for determining the expected yield from this management practice. By applying the 240 kg ha^{-1} N rate to grid cell #4, the producer could expect a 50:50 chance of yield greater than 9681 kg ha^{-1} in any given growing season. Similarly, the producer could expect an 80% chance of yield less than 11,333 kg ha^{-1} or a 20% chance of yield greater than 11,333 kg ha^{-1} (Fig. 5).

Given that the producer must apply 240 kg ha^{-1} of N in grid cell #4 to maximize average marginal net return over 37 growing seasons, the cumulative exponential probability distributions of unused N (Fig. 7) are now useful for determining the environmental risk associated with this management practice. The curve for an N rate of 240 kg ha^{-1} in grid cell #4 shows that there is a 50:50 chance that the amount of unused N left in the soil will be greater than 30.6 kg ha^{-1}. Similarly, there is an 80% probability that the amount of unused N left in the soil will be less than

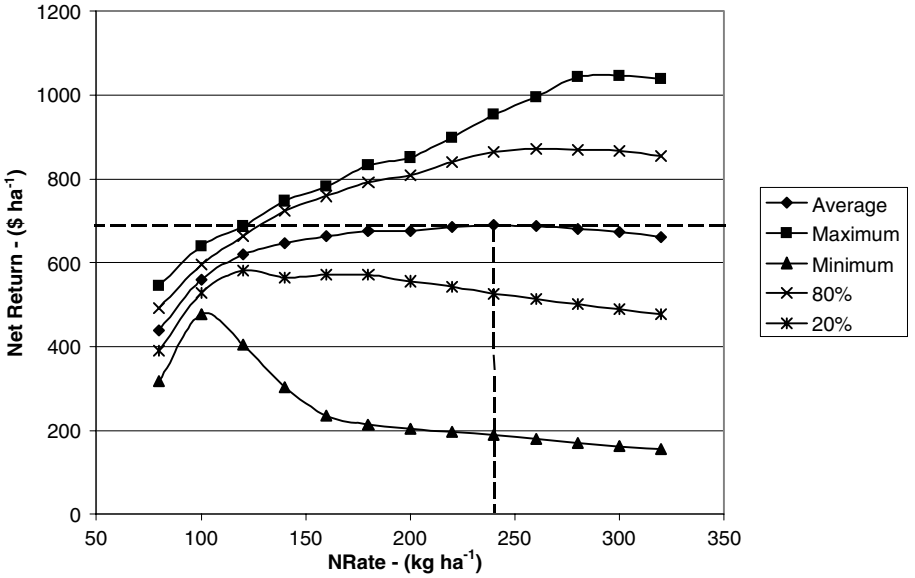

Fig. 8. The 240 kg ha^{-1} N rate maximizes average marginal net return in grid cell #4 over 37 growing seasons.

49.4 kg ha^{-1} or a 20% probability that unused N will be greater than 49.4 kg ha^{-1}. This represents the environmental risk associated with applying the 240 kg ha^{-1} N rate in grid cell #4, because N left unused in the soil will be highly susceptible to loss in the months between growing seasons. In terms of the quantity of N left unused in soil when optimizing producer economics, the grid cell #4 value of 49.4 kg ha^{-1} at the 80% probability level is relatively moderate, only slightly lower than the field average of 56.2 kg ha^{-1}. On the other hand, in grid cell #74, the N management practice that optimized marginal net return (260 kg ha^{-1} N) had an 80% chance of leaving 120.9 kg ha^{-1} or less of unused N in the soil at harvest. In other words, if N is managed to optimize economic return in this grid cell, nearly half of the applied N will remain in the soil after harvest in 20% of growing seasons.

By repeating this analysis for all 100 grid cells, an N prescription map was developed for optimizing marginal net return across the entire study area (Fig. 9). Since the model runs for the prescription analysis were performed with the assumption of nearly zero initial N in the soil, measurements of the actual available N in the soil prior to a fertilizer application should be used as a credit for the N rates given in this prescription. The average N rate to optimize production across all 100 grid cells was 233 kg ha^{-1} with a standard deviation of 21 kg ha^{-1} (Table 3). Based on the weather of the past 37 growing seasons, this variable-rate N prescription would have an 80% chance of producing a field average crop yield of 11,009 kg ha^{-1} or less with a standard deviation of 589 kg ha^{-1} across grid cells. Also, the management practice would have an 80% chance of leaving a field level average of 56.2 kg ha^{-1} or less unused N in the soil at harvest with a standard deviation of 16.7 kg ha^{-1} across grid cells.

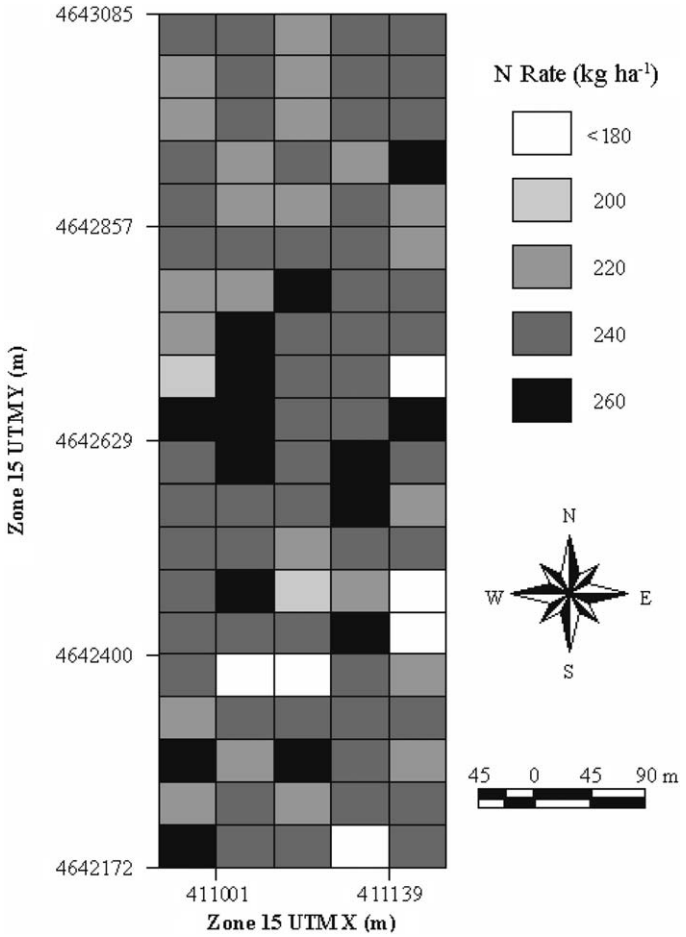

Fig. 9. Nitrogen prescription for optimizing marginal net return over 37 growing seasons.

Finally, this N prescription would have an 80% chance of achieving a field average marginal net return of less than \$839.44 ha^{-1} with a standard deviation of \$43.10 ha^{-1} over 100 grid cells.

4.2. Opportunity cost of environmental protection

Managing N to optimize marginal net return assures that producers can achieve the maximum possible profit from their corn crop. However, this practice can have significant environmental impacts in some areas of an agricultural field, because there is a greater chance that a large quantity of N will remain in the soil after harvest. To reduce the environmental impacts of corn production, producers must begin managing N to achieve a balance between environmental and production objectives. For example, assume that lawmakers establish an environmental policy stating that

Table 3
Field-level statistics over all 100 grid cells for the economically optimum prescription at the 80% probability threshold

	N rate (kg ha^{-1})	Yield (kg ha^{-1})	Unused N (kg ha^{-1})	Marginal net return ($ ha^{-1})
Average	233	11,009	56.2	839.44
Standard deviation	21	589	16.7	43.10
Minimum	160	8910	35.0	692.66
Maximum	260	11,816	120.9	896.58

unused N left in the soil after harvest must be less than 40 kg ha^{-1} 80% of the time. Cumulative exponential probability of unused N (Fig. 7) can now be used to determine the rate of N that will meet this objective for grid cell #4 of the study area. Furthermore, we can use cumulative beta probability of yield (Fig. 5) to determine the yield and the producer's opportunity cost (Eq. (9)), which is the profit that the producer foregoes by managing N to meet to the environmental restriction. With linear interpolation between the cumulative exponential probability curves for the 220 and 240 kg ha^{-1} N rates, an N rate of 222 kg ha^{-1} insures that the amount of unused N will be less than 40 kg ha^{-1} with a probability of 80% (Fig. 7). Then using the cumulative beta probability of yield curves, an N rate of 222 kg ha^{-1} will give a crop yield of 11,006 kg ha^{-1} 80% of the time (Fig. 5). The producer's opportunity cost for reducing N rates can now be calculated using Eq. (9). For grid cell #4, the producer's opportunity cost for leaving less than 40 kg ha^{-1} of unused N in the soil at harvest with a probability of 80% is $20.01 ha^{-1}.

By repeating this analysis for all 100 grid cells, an N prescription map was developed for meeting the environmental objective of leaving less than 40 kg ha^{-1} unused N in the soil at harvest with 80% probability across the entire study area (Fig. 10). Again, since the model runs for the prescription analysis were performed with the assumption of nearly zero initial N in the soil, measurements of the actual available N in the soil prior to a fertilizer application should be used to credit the N rates given in this prescription. The average N rate to accomplish the environmental objective across all 100 grid cells was 194 kg ha^{-1} with a standard deviation of 41 kg ha^{-1} (Table 4). Based on the weather of the past 37 growing seasons, this variable-rate N prescription would have an 80% chance of producing a field average crop yield of 10,240 kg ha^{-1} or less with a standard deviation of 1146 kg ha^{-1} across grid cells. Also, this management practice would have an 80% chance of achieving a field average marginal net return of less than $791.32 ha^{-1} with a standard deviation of $79.81 ha^{-1} over 100 grid cells. The field level average opportunity cost incurred by the producer using this precision N management strategy would be $48.12 ha^{-1} with standard deviation of $53.13 ha^{-1} across the 100 grid cells. At this cost, the average amount of N left unused in the soil at harvest would be reduced by greater than 16.2 kg ha^{-1} in 20% of growing seasons. Interestingly, in seven of the 100 grid cells the producer's opportunity cost was negative, indicating that the prescription for optimizing net return already leaves less than 40 kg ha^{-1} of unused N in soil with 80% probability. For these grid cells, the N rate that forces the environmental objective is actually greater than the

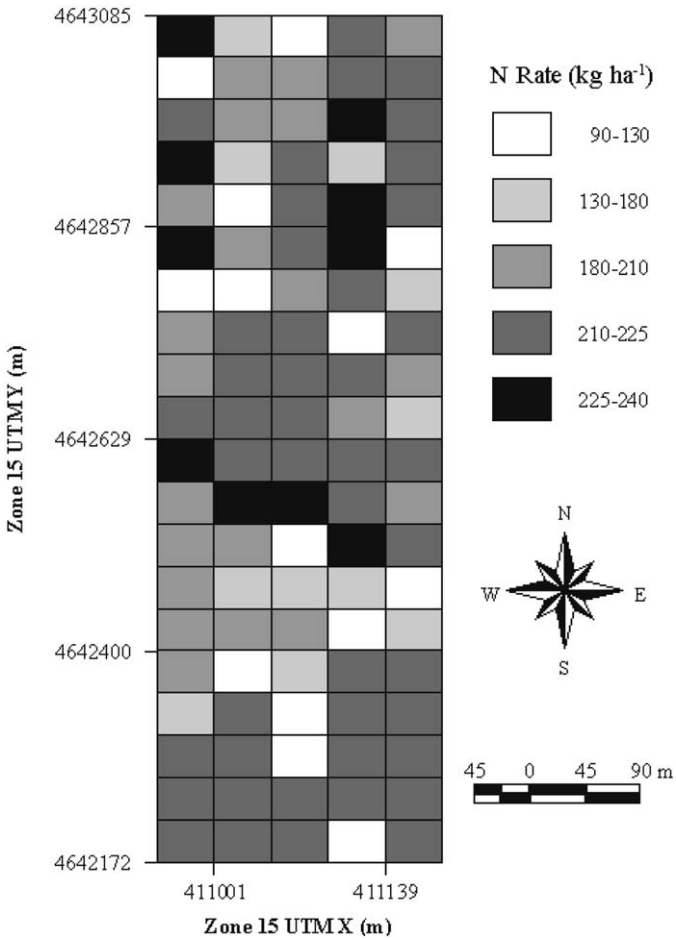

Fig. 10. Nitrogen prescription for not exceeding 40 kg ha^{-1} of unused N in the soil at harvest in 80% of growing seasons.

N rate that optimizes economic return. Obviously, the producer should use the economically optimal N rate for these grid cells. A map of the spatial distribution of opportunity cost demonstrates how an environmentally conscience management scenario for N fertilizer is quite costly to the producer in some areas of the field, but in other grid cells it costs the producer nothing (Fig. 11). As expected, the grid cells that require the lowest rates to meet the environmental objective (Fig. 10) also cost the producer significantly to manage in this way (Fig. 11).

The environmental policy of leaving no more than 40 kg ha^{-1} of unused N in the soil after harvest with 80% probability was picked at random for demonstration purposes. However, if such a strategy such were actually implemented to legislate requirements for agricultural N management, the future economic prosperity of

Table 4
Field-level statistics over all 100 grid cells for the environmental objective of no more than 40 kg ha^{-1} of unused N in the soil at harvest in 80% of growing seasons

	N rate (kg ha^{-1})	Yield (kg ha^{-1})	Unused N (kg ha^{-1})	Marginal net return ($ ha^{-1})	Opportunity cost ($ ha^{-1})
Average	194	10,240	40	791.32	48.12
Standard deviation	41	1146	0	79.81	53.13
Minimum	90	6778	40	541.13	−10.52
Maximum	238	11,383	40	869.70	246.65

the agricultural industry would depend heavily on a sound methodology for appropriately selecting the environmental restriction to be met. Inappropriate or unrealistic expectations could have severe effects on the economics of a farming operation.

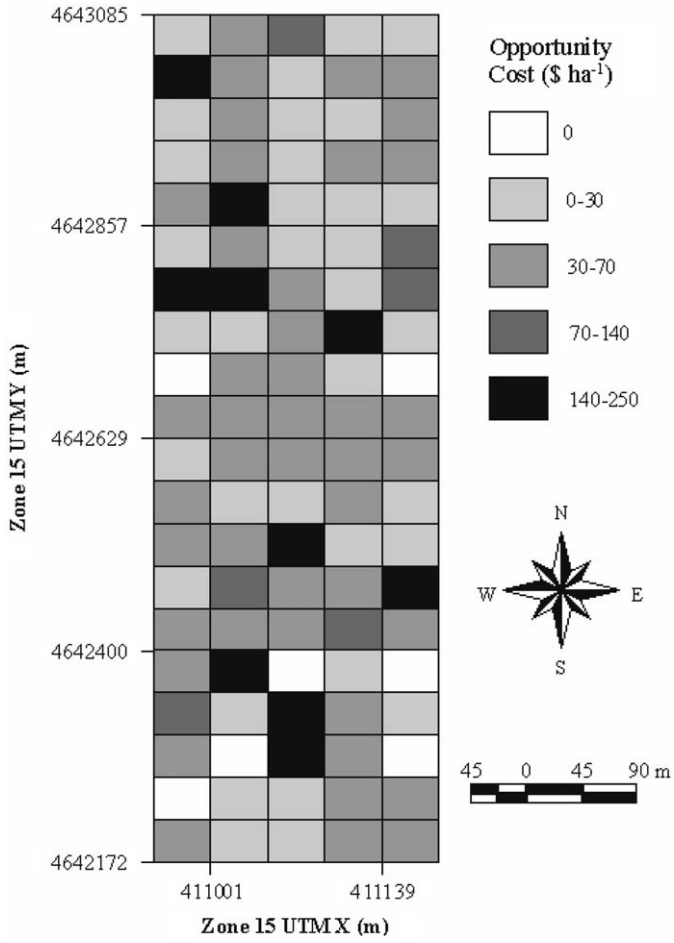

Fig. 11. Producer's opportunity cost for leaving less than 40 kg ha^{-1} of unused N in the soil 80% of the time.

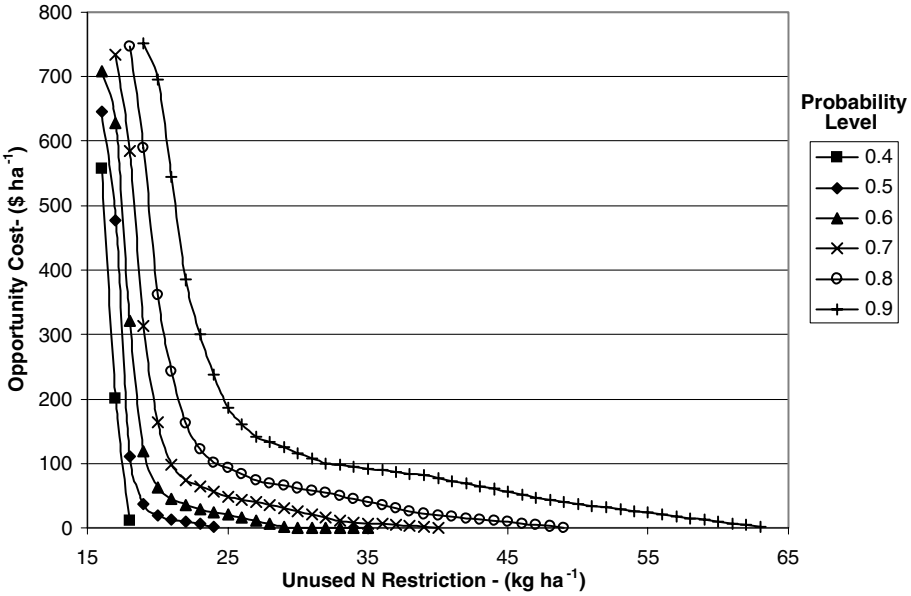

Fig. 12. Producer's opportunity cost in grid cell #4 for unused N restriction levels ranging from 15–65 kg ha^{-1} at six different levels of probability.

To aid in this policy making process, the probability curves can be manipulated to obtain the producer's opportunity cost for many possible environmental policy scenarios (Fig. 12). To develop the plot, the producer's opportunity cost was determined at several different probability levels while incrementing the restriction for unused N by one over the range of 15–65 kg ha^{-1}. This type of plot would give a policymaker a tool for judging the degree of impact that a particular policy, in terms of the restriction for unused N left in the soil, would have on a producer. For the previous example, an environmental restriction of no more than 40 kg ha^{-1} of unused N in the soil with 80% probability was implemented. Fig. 12 demonstrates that this scenario is relatively lenient for grid cell #4, since it costs the producer only \$20.01 ha^{-1} in that grid cell. However, if the environmental policy had been established to be no more than 20 kg ha^{-1} of unused N in the soil with 80% probability, the opportunity cost jumps to \$360.95 ha^{-1} in grid cell #4. Such a policy would not be economically feasible for the corn grower. Effective policies for restricting the amount of unused N in the soil after harvest must strive to achieve a proper balance between environmental risk and producer economics.

5. Conclusions

Precision management of N fertilizer has not become common practice in the midwestern United States, because the economic cost incurred by applying reduced N rates has not been adequately demonstrated. Such information has

been difficult to generate because the dynamics of N movement in an agricultural system is highly complex and because it varies depending on spatial location and weather patterns. Crop growth models can serve as a useful tool to make sense of this complex dynamic system. Given the soil properties, management practices, and historical weather information for specific study areas, model simulations are able to demonstrate how various N management scenarios would have affected yield and unused N in the soil at harvest under the weather conditions of past growing seasons. By fitting cumulative probability distributions to the yield and unused N data, simulation results from past growing seasons can be used to look forward in time, and the uncertainty associated with the effect of unknown future weather on future yield and future unused N left in the soil can be discussed in terms of probability. On the basis of chance, these probability distributions effectively unite yield and unused N left behind, the two most important variables for addressing the production and environmental concerns of N management in agricultural cropping systems.

References

Bakhsh, A., Kanwar, R.S., Karlen, D.L., Cambardella, C.A., Colvin, T.S., Moorman, T.B., Bailey, T.B., 2000. Tillage and nitrogen management effects on crop yield and residual soil nitrate. Transactions of the ASAE 43, 1589–1595.

Batchelor, W.D., Basso, B., Paz, J.O., 2002. Examples of strategies to analyze spatial and temporal yield variability using crop models. European Journal of Agronomy 18, 141–158.

Batchelor, W.D., Paz, J.O., Thorp, K.R., 2004. Development and evaluation of a decision support system for precision agriculture. In: Proceedings of the 7th International Conference on Precision Agriculture. ASA-CSSA-SSSA, Madison, WI, USA..

Blackmer, T.M., Schepers, J.S., Varvel, G.E., Meyer, G.E., 1996. Analysis of aerial photography for nitrogen stress within corn fields. Agronomy Journal 88, 729–733.

Burkart, M.R., James, D.E., 1999. Agricultural-nitrogen contributions to hypoxia in the Gulf of Mexico. Journal of Environmental Quality 28, 850–859.

Dinnes, D.L., Karlen, D.L., Jaynes, D.B., Kaspar, T.C., Hatfield, J.L., Colvin, T.S., Cambardella, C.A., 2002. Nitrogen management strategies to reduce nitrate leaching in tile-drained Midwestern soils. Agronomy Journal 94, 153–171.

Flowers, M., Weisz, R., Heiniger, R., Tarleton, B., Meijer, A., 2003. Field validation of a remote sensing technique for early nitrogen application decisions in wheat. Agronomy Journal 95, 167–176.

Gabrielle, B., Kengni, L., 1996. Analysis and field-evaluation of the CERES model's soil components: nitrogen transfer and transformations. Soil Science Society of America Journal 60, 142–149.

Gabrielle, B., Menasseri, S., Houot, S., 1995. Analysis and field evaluation of the CERES models water balance component. Soil Science Society of America Journal 59, 1403–1412.

Garrison, M.V., Batchelor, W.D., Kanwar, R.S., Ritchie, J.T., 1999. Evaluation of the CERES-Maize water and nitrogen balances under tile-drained conditions. Agricultural Systems 62, 189–200.

Gnanadesikan, R., Pinkham, R.S., Hughes, L.P., 1967. Maximum likelihood estimation of the parameters of the beta distribution from smallest order statistics. Technometics 9, 607–620.

Goolsby, D.A., Battaglin, W.A., Aulenbach, B.T., Hooper, R.P., 2001. Nitrogen input to the Gulf of Mexico. Journal of Environmental Quality 30, 329–336.

GopalaPillai, S., Tian, L., 1999. In-field variability detection and spatial yield modeling for corn using digital aerial imaging. Transactions of the ASAE 42, 1911–1920.

Jaynes, D.B., Colvin, T.S., 1997. Spatiotemporal variability of corn and soybean yield. Agronomy Journal 89, 30–37.

Johnson, N.L., Kotz, S., Balakrishnan, N., 1994. Continuous Univariate Distributions, vols. I and II. Wiley, New York, NY, USA.

Jones, C.A., Kiniry, J.R., 1986. CERES-Maize: A Simulation Model of Maize Growth and Development. Texas A&M University Press, College Station, TX, USA.

Katsvairo, T.W., Cox, W.J., Van Es, H.M., Glos, M., 2003. Spatial yield response of two corn hybrids at two nitrogen levels. Agronomy Journal 95, 1012–1022.

Kobayashi, K., Salam, M.U., 2000. Comparing simulated and measured values using mean squared deviation and its components. Agronomy Journal 92, 345–352.

Noh, H.K., Zhang, Q., Shin, B.S., Han, S., 2003. Multispectral image sensor for detection of nitrogen deficiency in corn using an empirical line method. ASAE Paper No. 031135. American Society of Agricultural Engineers, St. Joseph, MI, USA.

Paz, J.O., Batchelor, W.D., Babcock, B.A., Colvin, T.S., Logsdon, S.D., Kaspar, T.C., Karlen, D.L., 1999. Model-based technique to determine variable rate nitrogen for corn. Agricultural Systems 61, 69–75.

Press, W.H., Teukolsky, S.A., Vetterling, W.T., Flannery, B.P., 1992. Numerical Recipes in C: The Art of Scientific Computing. Cambridge University Press, New York, NY, USA.

Ratliff, L.F., Ritchie, J.T., Cassel, D.K., 1983. Field-measured limits of soil water availability as related to laboratory-measured properties. Soil Science of America Journal 47, 770–775.

Royston, P., 1995. A remark on Algorithm AS 181: The W-test for normality. Applied Statistics 44, 547–551.

Schepers, J.S., Francis, D.D., Vigil, M., Below, F.E., 1992. Comparison of corn leaf nitrogen concentration and chlorophyll meter readings. Communications of Soil Science and Plant Analysis 23, 2173–2187.

Schmidt, J.P., Dejoia, A.J., Ferguson, R.B., Taylor, R.K., Young, R.K., Harlin, J.L., 2002. Corn yield response to nitrogen at multiple in-field locations. Agronomy Journal 94, 798–806.

Searcy, S.W., Schueller, J.K., Bae, Y.H., Borgelt, S.C., Stout, B.A., 1989. Mapping of spatially variable yield during grain combining. Transactions of the ASAE 32, 826–829.

Shapiro, S.S., Wilk, M.B., 1965. An analysis of variance test for normality (complete samples). Biometrika 52, 591–611.

Thorp, K.R., Batchelor, W.D., and Paz, J.O., 2005a. Programming ArcGIS to generate crop model input files for spatial simulations. ASAE Paper No. 053012. American Society of Agricultural Engineers, St. Joseph, MI, USA.

Thorp, K.R., Batchelor, W.D., and Paz, J.O., 2005b. A cross validation approach to evaluate CERES-Maize simulations of corn yield spatial variability. ASAE Paper No. 053002. American Society of Agricultural Engineers, St. Joseph, MI, USA.

USDA-SCS, 1981. Soil Survey of Boone County, Iowa. United States Department of Agriculture–Soil Conservation Service (USDA-SCS), Iowa Agriculture and Home Economics Experiment Station Cooperative Extension Service, Iowa State University, and State of Iowa Department of Soil Conservation, Ames, IA, USA.